Journal of Power Sources 195 (2010) 1757–1760

Contents lists available at ScienceDirect

Journal of Power Sources

journal homepage: www.elsevier.com/locate/jpowsour

Short communication

Electrochemical capacitance of Co_3O_4 nanowire arrays supported on nickel foam

Yinyi Gao, Shuli Chen, Dianxue Cao*, Guiling Wang, Jinling Yin

College of Material Science and Chemical Engineering, Harbin Engineering University, Natong St #145, Harbin 150001, PR China

ARTICLE INFO

Article history:
Received 31 July 2009
Received in revised form
25 September 2009
Accepted 27 September 2009
Available online 3 October 2009

Keywords:
Cobalt oxide
Nanowire arrays
Capacitance
Supercapacitor

ABSTRACT

Co_3O_4 nanowire arrays freely standing on nickel foam are prepared via template-free growth followed by thermal treatment at 300 °C in air. Their morphology is examined by scanning and transmission electron microscopy. The electrochemical capacitance behavior of the self-supported binderless nanowire array electrode is investigated by cyclic voltammetry, galvanostatic charge–discharge test and electrochemical impedance spectroscopy. The results show that nanowires are formed by nanoplatelets packed roughly layer by layer. They densely cover the nickel foam substrate and have diameters around 250 nm and the lengths up to around 15 μm. The Co_3O_4 nanowires display a specific capacitance of 746 F g^{-1} at a current density of 5 mA cm^{-2}. The capacitance loss is less than 15% after 500 charge–discharge cycles. The columbic efficiency is higher than 93%.

1. Introduction

Electrochemical capacitors (supercapacitors) have high power density, long charge–discharge cycle life and high energy efficiency. The combined system of supercapacitors and rechargeable batteries or fuel cells is considered to be a potential power source for electric vehicles. In this system, supercapacitors provide the necessary high power for acceleration and allow for recuperation of brake energy [1]. The development of high performance electrode materials for supercapacitors has attracted increased interests in recent years and three major types of electrode materials are reported, including carbon, metal oxides, and conducting polymers [2–4]. Out of the metal oxides, cobalt oxides and hydroxides are reported to be promising electrode materials for supercapacitors because of their high redox activity and great reversibility [5–23]. The theoretical specific capacitance of Co_3O_4 is 3560 F g^{-1} [5]. Very recently, by using an entirely electrochemical process, Deng et al. successfully prepared a nano-structured cobalt oxide electrode, which shows a specific capacitance as high as 2200 F g^{-1} measured at a potential scan rate of 10 mV s^{-1} [5]. Zhou et al. prepared novel ordered mesoporous cobalt hydroxide films on a foamed Ni substrate by electrodeposition and found the film electrode has a maximum specific capacitance of 2646 F g^{-1} [18]. These nano-structured cobalt oxides and hydroxides displayed much higher capacitance than their conventional bulk counterparts, demonstrating that nanostructure has significant effects on the capacitance performance of the active electrode materials. Nano-structured electrodes provide large surface area and lead to a high utilization of materials because pseudo-capacitors store charges in the first few nanometers from the surface.

Co_3O_4 nanowire arrays supporting on conducting substrates (serving as the current collector) or on solid electrolyte membrane have been synthesized using template-free or virus-templated methods [24–27]. These Co_3O_4 nanowires displayed high capacity and rate capability as the anode material for Li-ion batteries. The reversible capacity reached around 700 mAh g^{-1}, which is twice of that of current graphite anode. Our recent study showed that nickel foam supported Co_3O_4 nanowire array electrode exhibited better performance for H_2O_2 electroreduction in terms of both activity and mass transport property than conventional nanoparticle Co_3O_4/carbon/PTFE electrode [28]. The superior performance results from the unique nano-structure of the electrode, which make the electrode have large surface area per unit volume, high utilization of the active material, and excellent mass transport property.

In this study, Co_3O_4 nanowire arrays supported on nickel foam substrate were prepared via a template-free synthesis method. Their electrochemical capacitance behavior in KOH solution was investigated. This self-supported binderless nanowire array electrode showed much higher specific capacitance than conventional electrode made of Co_3O_4 nanowires or nanoparticles, conducting carbon and PTFE binder.

2. Experimental

Co_3O_4 nanowire arrays supported on nickel foam were prepared via a template-free growth method [24,25,28]. Briefly, 12 mmol $Co(NO_3)_2$ and 6 mmol NH_4NO_3 were dissolved in a solu-

* Corresponding author. Tel.: +86 451 82589036; fax: +86 451 82589036.
E-mail address: caodianxue@hrbeu.edu.cn (D. Cao).

0378-7753/$ – see front matter © 2009 Elsevier B.V. All rights reserved.
doi:10.1016/j.jpowsour.2009.09.048

tion consisting of 35 cm^3 H_2O and 15 cm^3 ammonia (30 wt%). The solution was magnetically stirred for 10 min in air at room temperature and heated at 90 ± 1 °C for 2 h in an oven. This solution is ready for nanowire growth. A piece of nickel foam (10 mm × 10 mm × 1.1 mm, 110 PPI, 320 g m^{-2}, Changsha Lyrun Material Co., Ltd. China) was degreased with acetone, etched with 6.0 mol dm^{-3} HCl for 5 min, rinsed with water, soaked in 0.1 mmol dm^{-3} $NiCl_2$ solution for 4 h, rinsed again with water extensively, and immersed in the growing solution for 14 h at 90 ± 1 °C to allow growth of nanowires. The nickel foam covered with nanowires was washed with H_2O, dried at room temperature for 6 h, and then heated at 300 °C for 2 h in air to obtain the final electrode. The 1 cm^2 electrode contains 16 mg Co_3O_4 nanowires. The morphology was examined by scanning electron microscope (SEM, JEOL JSM-6480) and transmission electron microscope (TEM, FEI Teccai G2 S-Twin, Philips).

Electrochemical measurements were performed in a conventional three-electrode electrochemical cell using a computerized potentiostat (Autolab PGSTAT302, Eco Chemie) controlled by GPES software. The nickel foam supported nanowire arrays acted as the working electrode. A blackened Pt gauze behind a D-porosity glass frit was employed as the counter electrode. A saturated calomel electrode (SCE) served as the reference. All potentials were referred to the reference electrode. All electrochemical measurements were performed at room temperature in aqueous KOH solution. All solutions were made with analytical grade chemical reagents and Millipore Milli-Q water (18 MΩ cm). Electrochemical impedance spectroscopy (EIS) measurements were carried out by applying an AC voltage with 5 mV amplitude in a frequency range from 0.01 Hz to 100 kHz at open circuit potential.

3. Results and discussion

3.1. Characterization of the Co_3O_4 nanowire array electrode

Fig. 1A and B shows the SEM image of the Co_3O_4 nanowire arrays attached on nickel foam skeleton and the TEM image of a single nanowire scratched down from the nickel foam, respectively. The nanowires densely covered the nickel foam substrate and have relatively uniform size. The diameter is around 250 nm and the length is up to around 15 μm. TEM shows that the nanowire is formed by nanoplatelets packed roughly layer by layer (Fig. 1B). SEM shows that the nanowires grow in random direction and cross each other (Fig. 1A). This growth pattern differs from that reported by Li et al. and our group [24,25,28]. These previous study demonstrated that Co_3O_4 nanowires grow almost vertically from the surface of substrate, e.g., Si, Ti and foamed Ni. The difference probably results from the different nanowire growth condition. In this study, higher concentration of $Co(NO_3)_2$ and NH_4NO_3 and longer growth time than previous studies were used in order to obtain higher Co_3O_4 nanowire loading (16 mg cm^{-2} in this study vs. around 8 mg cm^{-2} in previous studies) [28]. We have demonstrated in our previous study, by X-ray diffraction, infrared spectroscopy and thermal gravimetric analysis, that the nanowires are pure spinel Co_3O_4 [28].

3.2. Electrochemical properties of the Co_3O_4 nanowire array electrode

Fig. 2 shows the cyclic voltammograms (CV) of Co_3O_4 nanowire arrays recorded in 6.0 mol dm^{-3} KOH solution at different scan rates between 5 and 50 mV s^{-1}. Two pairs of redox peaks were observed at 5 mV s^{-1} scan rate, which correspond to the conversion between different cobalt oxidation states according to the following equations [5,7,29]:

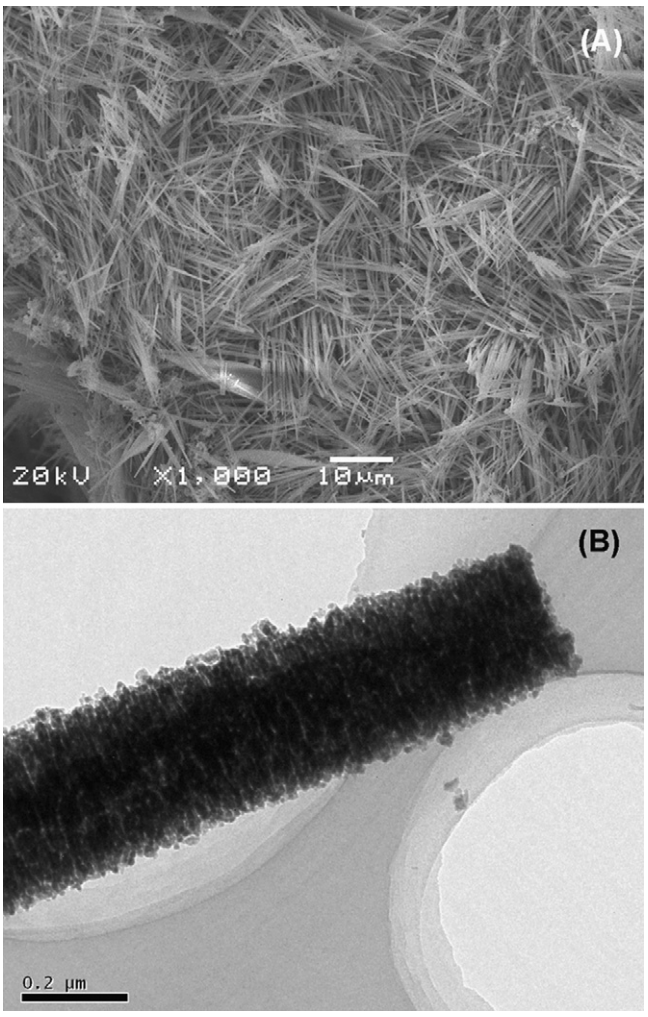

Fig. 1. The SEM image of the Co_3O_4 nanowire arrays attached on nickel foam skeleton (A) and the TEM image of a single nanowire scratched down from the nickel foam (B).

$$Co_3O_4 + OH^- + H_2O \Leftrightarrow 3CoOOH + e^- \quad (1)$$

$$CoOOH + OH^- \Leftrightarrow CoO_2 + H_2O + e^- \quad (2)$$

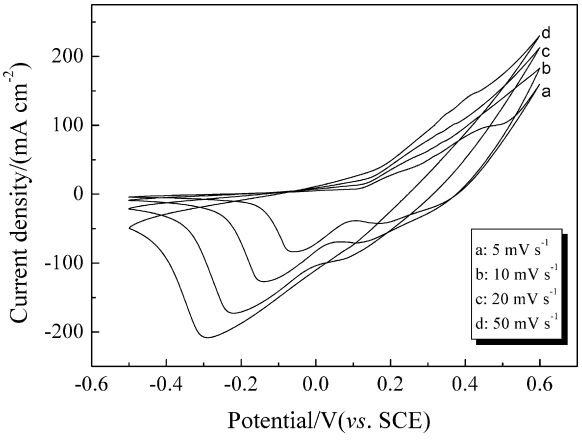

Fig. 2. Cyclic voltammograms of Co_3O_4 nanowire arrays recorded in 6.0 mol dm^{-3} KOH solution at different scan rates between 5 and 50 mV s^{-1}.

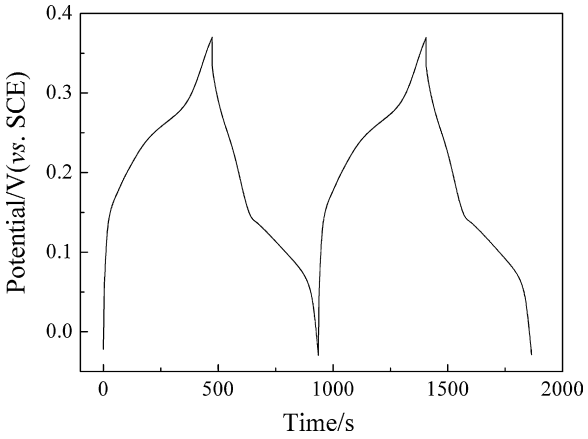

Fig. 3. The first and second charge–discharge curves of the Co_3O_4 nanowire array electrode in 6.0 mol dm^{-3} KOH solution at a galvanostatic current density of 10 mA cm^{-2}.

With the increase of the scan rate, anodic peaks overlapped and cathodic peaks shifted toward negative potential, indicating the quasi-reversible feature of the redox couples. The large difference between the anodic and cathodic peak potential is likely related to the low electronic conductivity of the long nanowires because no conducting carbon were used in this electrode. Fig. 3 shows the first and second charge–discharge curves of the Co_3O_4 nanowire array electrode in 6.0 mol dm^{-3} KOH solution at a galvanostatic current density of 10 mA cm^{-2} (0.624 A g^{-1}) in the potential range of −0.05 to 0.38 V. The discharge curve consists of two sections, a sudden potential drop followed by a slow potential decay. The first potential drop results from the internal resistance and the subsequent potential decay represents the capacitive feature of the electrode. The obvious deviation of the shape of the discharge curves from straight line (Fig. 3) and the shape of CV from the ideal rectangular shape (Fig. 2) revealed that the pseudo-capacitance is not pure double-layer capacitance, but faradic capacitance, which mainly originates from the redox reaction.

Fig. 4 shows the discharge curves of the Co_3O_4 nanowire array electrode measured at different discharge current densities within the potential window of 0–0.35 V in 6.0 mol dm^{-3} KOH solution. The specific capacitance can be calculated according to the following equation:

$$C_m = \frac{I_d \times \Delta t}{\Delta V \times m} \quad (3)$$

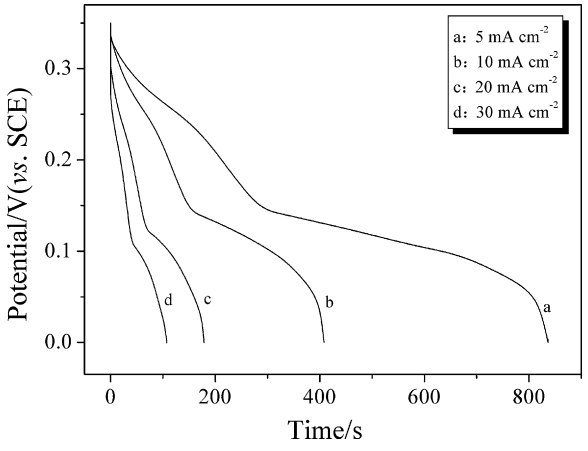

Fig. 4. The discharge curves of the Co_3O_4 nanowire array electrode measured at different discharge current densities in 6.0 mol dm^{-3} KOH solution.

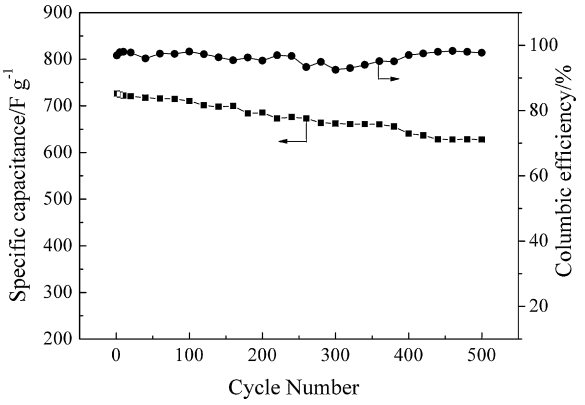

Fig. 5. Dependences of the discharge specific capacitance and the columbic efficiency on the charge–discharge cycle numbers. The charge–discharge tests were performed at 10 mA cm^{-2} in 6.0 mol dm^{-3} KOH solution.

where C_m (F g^{-1}) is the specific capacitance, I_d (mA) is the discharge current, Δt (s) is the discharge time, ΔV (V) is the potential change during discharge, and m (mg) is the mass of the active material within the electrode (16 mg). The specific capacitance values of the Co_3O_4 nanowires evaluated from the discharge curves are 746, 727, 639, and 568 F g^{-1} at the current density of 5, 10, 20, and 30 mA cm^{-2}, respectively. Such large values of capacitance can be attributed to the unique porous nano-structure and the large specific surface area of the nanowires [24]. These capacitances are much higher than that of Co_3O_4 nanowire array prepared using the anodic alumina oxide template method [9]. The decrease of the capacitance with the increase of the discharge current density is likely caused by the increase of potential drop due to the resistance of the nanowires and the relatively insufficient Faradic redox reaction of the active material under higher discharge current densities. The specific capacitance obtained at the slowest scan rate is more close to that of full utilization of the active material of the electrode.

Fig. 5 shows the dependence of the discharge specific capacitance and the columbic efficiency of the electrode on the charge–discharge cycle numbers. The charge–discharge experiments were performed at a current density of 10 mA cm^{-2} within the potential window of 0 to 0.35 V in 6.0 mol dm^{-3} KOH solution. The columbic efficiency was calculated using the following equation:

$$\eta = \frac{t_d}{t_c} \times 100 \quad (4)$$

where t_c and t_d represent the time of charge and discharge, respectively.

As shown in Fig. 5, the discharge specific capacitance decreased to 86% after 500 cycles, indicating that nanowire electrode has relatively good electrochemical stability. The columbic efficiency ranged from 93% to 98%. The repetitive charge–discharge cycling does not induce noticeable changes of the nanowire structure. Resistance is an important aspect of a supercapacitor electrode, which was investigated by electrochemical impedance spectroscopy analysis. Fig. 6 shows the Nyquist plots of Co_3O_4 nanowire array electrode before and after charge–discharge cycling measured at open circuit potential in 6.0 mol dm^{-3} KOH solution. The spectrum measured before charge–discharge displays a semicircle at high frequency region and straight lines with slope of 52° and 72° at low frequency region. The semicircle is related to Faradic reactions. The 52° straight line corresponds to a Warburg impedance related to the diffusion of electrolyte within the pores of the electrode. The 72° straight line shows the capacitance nature (vertical line for an ideal capacitor). This EIS profile is typical for an electrochemical capacitor [1]. After 500 charge–discharge cycles, the EIS

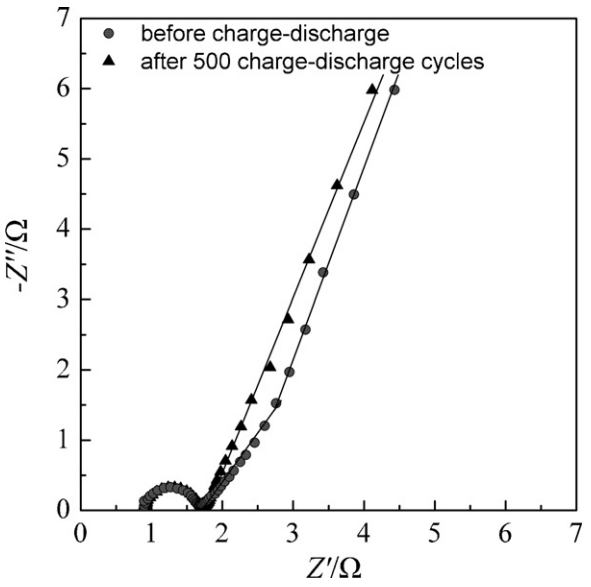

Fig. 6. Electrochemical impedance spectra of Co_3O_4 nanowire array electrode before and after charge–discharge cycling.

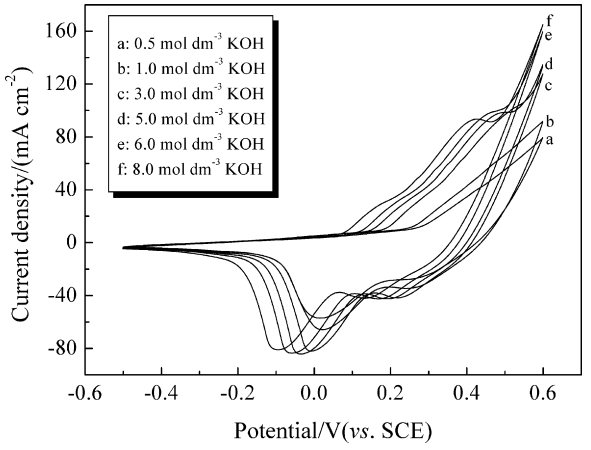

Fig. 7. Cyclic voltammograms of the nanowire array electrode in KOH electrolyte of different concentrations at a scan rate of 5 mV s^{-1}.

spectrum only shows a semicircle at high frequency region and a 72° straight line at low frequency region. The charge transfer resistance is about 0.75 Ω before charge–discharge and remains nearly unchanged after 500 charge–discharge cycles. These results demonstrated the good electrochemical stability and the pseudo-capacitance characteristics of the nanowire array electrode.

The effect of concentration of KOH electrolyte was investigated by cyclic voltammetry. Fig. 7 shows the cyclic voltammograms of the nanowire array electrode at the scan rate of 5 mV s^{-1} within the potential range of −0.5 to 0.6 V in KOH electrolyte of different concentrations between 0.5 and 8.0 mol dm^{-3}. As the figure shows, the anodic currents increased with the increase of the concentration of KOH electrolyte, indicating the increase of specific capacitance with the increase of KOH solution. The voltammograms were more distorted at low electrolyte concentration. When the concentration of KOH is lower than 1.0 mol dm^{-3}, the CV did not show well-resolved anodic peaks. As the concentration of the electrolyte was increased to higher than 1.0 mol dm^{-3}, two anodic peaks started to be seen and their resolution improved with the KOH concentration increase. Clearly, the use of high concentration KOH benefits the capacitance, which can be attributed to the decrease of the electrolyte starvation near the nanowire surface and the reduction of internal resistance effect at high concentration electrolyte.

4. Conclusions

Co_3O_4 nanowire arrays supported on nickel foam were successfully prepared by a simple template-free method. The nickel foam having three-dimensional network structures serves both the support of Co_3O_4 nanowires and the current collector of the electrode, which makes the electrodes have large surface area and eliminates the use of ancillary conducting material and binder. The open spaces between neighboring nanowires allow for easy diffusion of electrolyte into the inner region of the electrode, resulting in reduced internal resistance and improved capacitance performance. Each nanowire has its own contact with the nickel foam current collector ensuring all nanowires participate in the electrochemical reaction, and thus enhanced the utilization of active materials. A specific capacitance of 746 F g^{-1} at a current density of 5 mA cm^{-2} is achieved ascribed to the unique nano-structure of the electrode.

Acknowledgements

We gratefully acknowledge the financial support of this research by National Nature Science Foundation of China (20973048), Heilongjiang Provincial Natural Science Foundation (ZJG2007-06-02), Key Laboratory of Superlight Materials and Surface Technology of Ministry of Education, and Harbin Engineering University (HEUFT07030, HEUFT07051 and HEUFT08008).

References

[1] R. Kotz, M. Carlen, Electrochim. Acta 45 (2000) 2483.
[2] P. Simon, Y. Gogotsi, Nat. Mater. 7 (2008) 845.
[3] Y. Zhang, H. Feng, X. Wu, L. Wang, A. Zhang, T. Xia, H. Dong, X. Li, L. Zhang, Int. J. Hydrogen Energy 34 (2009) 4889.
[4] A. Burke, Electrochim. Acta 53 (2007) 1083.
[5] M.J. Deng, F.L. Huang, I.W. Sun, W.T. Tsai, J.K. Chang, Nanotechnology 20 (2009) 175602.
[6] Y. Shan, L. Gao, Mater. Chem. Phys. 103 (2007) 206.
[7] C. Lin, J.A. Ritter, B.N. Popov, J. Electrochem. Soc. 145 (1998) 4097.
[8] L. Cao, M. Lu, H.L. Li, J. Electrochem. Soc. 152 (2005) A871.
[9] G. Ji, Z. Gong, W. Zhu, M. Zheng, S. Liao, K. Shen, J. Liu, J. Cao, J. Alloys Compd. 476 (2009) 579.
[10] V.R. Shinde, S.B. Mahadik, T.P. Gujar, C.D. Lokhande, Appl. Surf. Sci. 252 (2006) 7487.
[11] S.G. Kandalkar, J.L. Gunjakar, C.D. Lokhande, Appl. Surf. Sci. 254 (2008) 5540.
[12] H.J. Ahn, T.Y. Seong, J. Alloys Compd. 478 (2009) L8.
[13] E. Hosono, S. Fujihara, I. Honma, M. Ichihara, H. Zhou, J. Power Sources 158 (2006) 779.
[14] C. Yuan, X. Zhang, B. Gao, J. Li, Mater. Chem. Phys. 101 (2007) 148.
[15] V. Gupta, T. Kusahara, H. Toyama, S. Gupta, N. Miura, Electrochem. Commun. 9 (2007) 2315.
[16] H.K. Kim, T.Y. Seong, J.H. Lim, W.I. Cho, Y.S. Yong, J. Power Sources 102 (2001) 167.
[17] V. Srinivasan, J.W. Weidner, J. Power Sources 108 (2002) 15.
[18] W.J. Zhou, M.W. Xu, D.D. Zhao, C.L. Xu, H.L. Li, Micropor. Mesopor. Mater. 117 (2009) 55.
[19] T.C. Liu, W.G. Pell, B.E. Conway, Electrochim. Acta 44 (1999) 2829.
[20] L. Cao, F. Xu, Y.Y. Liang, H.L. Li, Adv. Mater. 16 (2004) 1853.
[21] S.G. Kandalkar, C.D. Lokhande, R.S. Mane, S.-H. Han, Appl. Surf. Sci. 253 (2007) 3952.
[22] Y. Wang, W. Yang, C. Chen, D.G. Evans, J. Power Sources 184 (2008) 682.
[23] V. Gupta, S. Gupta, N. Miura, J. Power Sources 177 (2008) 685.
[24] Y. Li, B. Tan, Y. Wu, Nano Lett. 8 (2008) 265.
[25] Y. Li, B. Tan, Y. Wu, J. Am. Chem. Soc. 128 (2006) 14258.
[26] K.T. Nam, D.W. Kim, P.J. Yoo, C.Y. Chiang, N. Meethong, P.T. Hammond, Y.M. Chiang, A.M. Belcher, Science 312 (2006) 885.
[27] G. Marbán, I. Lópeza, T. Valdés-Solís, A.B. Fuertesa, Int. J. Hydrogen Energy 33 (2008) 6687.
[28] G. Wang, D. Cao, C. Yin, Y. Gao, J. Yin, L. Cheng, Chem. Mater. (2009), doi:10.1021/cm901928b.
[29] C. Barbero, G.A. Planes, M.C. Miras, Electrochem. Commun. 3 (2001) 113.